

Superhard Cubic BC₂N Compared to Diamond

Yi Zhang,¹ Hong Sun,^{1,2} and Changfeng Chen²

¹*Department of Physics, Shanghai Jiao Tong University, Shanghai 200030, China*

²*Department of Physics and High Pressure Science and Engineering Center, University of Nevada, Las Vegas, Nevada 89154, USA*

(Received 7 May 2004; published 4 November 2004)

Recent experiments claimed successful synthesis of cubic boron-carbonitride compounds BC₂N with an extreme hardness second only to diamond. In the present Letter, we examine the ideal strength of cubic BC₂N using first-principles calculations. Our results reveal that, despite the large elastic parameters, compositional anisotropy and strain dependent bonding character impose limitation on their strength. Consequently, the hardness of the optimal BC₂N structure is predicted to be lower than that of cubic BN, the second hardest material known. The measured extreme hardness of BC₂N nanocomposites is most likely due to the nanocrystalline size effect and the bonding to the surrounding amorphous carbon matrix. This may prove to be a general rule useful in the quest for new superhard covalent materials.

DOI: 10.1103/PhysRevLett.93.195504

PACS numbers: 62.20.-x, 63.20.Dj, 71.15.Mb

The close similarity in the phase diagram and structural characteristics of diamond and cubic BN has led to the anticipation that zinc-blende-structured cubic boron-carbonitride (c-BCN) may form new superhard and superabrasive materials. Considerable efforts have been made in recent years to synthesize [1–5] and describe [6–10] possible c-BCN structures. Two recent experiments have reported [4,5] successful synthesis of a cubic BC₂N phase that is harder than cubic BN, the second (to diamond) hardest material known. This claim has been corroborated by the calculated [10] bulk modulus and shear moduli of BC₂N that exceed those of cubic BN; it was further supported by a recently developed empirical theory [11]. However, a closer examination of the situation reveals that several crucial issues need more careful investigation before this new order in material hardness can be declared. On the experimental side, the nanoindentation hardness measurements [4,5] were made on cubic BC₂N nanocomposites; the measured hardness is not expected to directly reflect that of the pure BC₂N phase. In view of this, it is important that theoretical studies establish accurate results on the mechanical strength for pure BC₂N phases. On the theoretical side, it is known that bulk and shear moduli do not necessarily give an accurate account for material hardness. This is because these elastic parameters are evaluated at the equilibrium structure, and material deformation associated with the hardness measurement occurs at finite strains where bonding characteristics may change significantly. Empirical formulations based on equilibrium charge and bond densities may fail for the same reason. A more stringent test is provided by the ideal strength, i.e., the stress at which a perfect crystal becomes mechanically unstable [12,13], that sets an upper bound for material strength.

In this Letter, we report on the first study of the ideal strength of cubic BC₂N and cubic BN using first-principles total-energy calculations. The stresses along various inequivalent crystallographic directions are evaluated to determine the weakest link that sets the limit on material strength. In addition, we carry out dynamic phonon calculations to search for possible inhomogeneous deformations that have been shown to be important for understanding anomalous material hardness [14–16]. The calculated results demonstrate that the hardest cubic BC₂N phase has an ideal strength that is appreciably lower than that of cubic BN. The effects of the nanocrystalline size and the bonding with the amorphous carbon matrix in BC₂N nanocomposites likely play a crucial role in producing the extreme hardness measured in experiments. The present results provide important insights into the atomistic origin of the structural deformation mechanisms and the limits they impose on the strength of cubic BC₂N.

The total-energy calculations have been carried out using the local-density-approximation (LDA) pseudo-potential scheme with a plane-wave basis set [17–19]. The norm-conserving Troullier-Martins pseudopotentials [20] were used with cutoff radii of 1.3, 1.3, and 1.5 a.u. for N, C, and B, respectively. The exchange-correlation functional of Ceperley and Alder [18] as parametrized by Perdew and Zunger [21] was used. The total energy of the structures was minimized by relaxing the structural parameters using a quasi-Newton method [22]. The total-energy and stress calculations used an eight-atom zinc-blende-structured unit cell, an 8 × 8 × 8 Monkhorst-Pack [23] *k*-point grid, and an 80 Ry energy cutoff. The error in the calculated stresses due to the energy cutoff and *k*-point grid was less than 0.1 GPa based on convergence tests. The quasistatic ideal

tensile strength and relaxed loading path in the various directions was determined using a method described previously [24,25]. The lattice vectors were incrementally deformed in the direction of the applied stress. At each step the structure was relaxed such that all the components of the Hellmann-Feynman stress tensor orthogonal to the applied stress were less than 0.1 GPa. Phonon modes of the crystal structure were calculated with the linear response theory using the ABINIT code [26].

For the eight-atom BC_2N unit cell there are a total of $8!/(2!)^4! = 420$ different configurations. Fortunately, only seven configurations are topologically different due to the high symmetry of the zinc-blende-structured lattice [10]. We have performed detailed calculations for all seven structures with a rich variety of local chemical bonding environments which play a crucial role in determining their ideal strength. Below we will present results for five cubic BC_2N structures, numbered one through five. Of the two structures left out, BC_2N-6 has very similar characteristics as BC_2N-5 and BC_2N-7 has the lowest density and is unstable due to phonon softening [27].

It has been shown [28] that the dominant failure mode in diamond is tensile in nature and the $\langle 111 \rangle$ direction is the weakest link that sets the limit on the ideal strength and hardness. This is also expected to be the case in cubic BN and BC_2N that have similar structural and bonding characters. We have calculated tensile strengths for all three materials. The results are 223.3, 126.3, and 92.8 GPa in $\langle 001 \rangle$, $\langle 011 \rangle$, and $\langle 111 \rangle$ directions, respectively, for diamond; these are in excellent agreement with previous calculations [28]. The corresponding data are 195.0, 94.0, and 65.0 GPa for cubic BN and 153.3, 80.1, and 55.7 GPa for BC_2N-2 (the same order found for all other BC_2N phases). Consequently, we will focus below on tensile stresses in the $\langle 111 \rangle$ direction for the ideal strength analysis. We have also calculated the ideal shear strength for all three materials in the weakest sliding planes. The results are 96.3 GPa for diamond, in excellent agreement with previous data [29], 70.5 GPa for c-BN, 68.8 GPa for BC_2N-2 , and 42.1 GPa for BC_2N-1 . Since the tensile strengths are lower than the shear strengths in all BC_2N phases, the deformation/failure of the tensile type will be dominant (or easier) under general loading conditions. Moreover, lower in *both* shear and tensile strengths compared to cubic BN means cubic BC_2N should be less hard. We present below a detailed analysis of the bonding characters in cubic BC_2N .

In Fig. 1 we present the calculated stress-strain results for diamond, cubic BN, and the two lowest-energy BC_2N phases. Several interesting features are noticed: (i) the lowest-energy BC_2N-1 , which has been almost exclusively used in previous studies of cubic BC_2N [6–10], shows significant anisotropy in stresses along different body diagonal directions. The ratio of the larger (in the

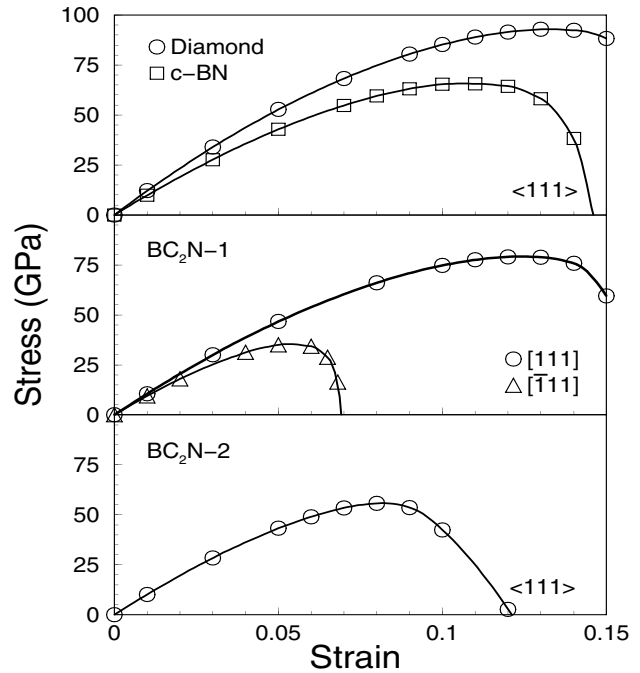


FIG. 1. The calculated tensile stresses in the body diagonal directions for diamond, cubic BN (c-BN) and two lowest-energy cubic BC_2N phases, BC_2N-1 and BC_2N-2 , with different local bonding environments (see Fig. 2). The results for diamond, c-BN, and BC_2N-2 are isotropic in all $\langle 111 \rangle$ directions, while those for BC_2N-1 are highly anisotropic.

$[111]$ and $[1\bar{1}1]$ directions) and smaller (in the $[\bar{1}11]$ and $[11\bar{1}]$ directions) peak stresses is $79.1/35.0 \text{ GPa} = 2.26$. The lower value of 35.0 GPa means this structure cannot be a superhard material as previously suggested [11]. (ii) the initial slope of the stress-strain curve (up to 1% strain) for BC_2N-1 is isotropic and the value is even slightly higher than that of cubic BN. However, at larger strains the stress in the $[\bar{1}11]$ direction quickly weakens and a breakdown results at about 6% strain. This strain dependent bonding character highlights the deficiency of common criteria for material hardness prediction using structural (bonding) characters at or near equilibrium. Quantities such as bulk and shear moduli or equilibrium bond and charge densities can lead to significant overestimates of hardness [11]. This is because the structural deformation associated with the hardness measurement occurs at finite (large) strain and the rise of the stress usually slows down with increasing strain. (iii) we find that BC_2N-2 , which is energetically almost degenerate with BC_2N-1 but has subtle differences in local bonding structures, demonstrates better overall strength. Although its maximum stress is not as high as that of BC_2N-1 in the $[111]$ direction, its stress-strain results are isotropic in all $\langle 111 \rangle$ directions. The peak stress of 55.7 GPa makes it the highest-strength BC_2N structure (see below), which should place it as the third hardest pure phase material after only diamond and cubic BN, which have ideal

strengths (in $\langle 111 \rangle$ directions) of 92.8 GPa and 65.6 GPa, respectively.

To examine the mechanisms and trends for structural deformation in cubic BC_2N , we have carried out detailed stress-strain and bond-length-strain calculations. Results in the direction with the minimum peak stress in each case are presented in Fig. 2. It is seen that the N-C bond is the weakest link and breaks up first under strain in all cases except for $\text{BC}_2\text{N-5}$, which contains broken N-N bonds [10]. In $\text{BC}_2\text{N-1}$, the weaker N-C and B-C bonds are all aligned in the $[\bar{1}\bar{1}\bar{1}]$ (and the equivalent $[1\bar{1}\bar{1}]$) direction while the stronger C-C and B-N bonds are all in the $[111]$ (and $[1\bar{1}\bar{1}]$) direction. This explains the large anisotropy in the ideal strength in $\text{BC}_2\text{N-1}$. In $\text{BC}_2\text{N-2}$, different bonds are evenly distributed in all $\langle 111 \rangle$ directions, leading to the isotropic strength distribution. $\text{BC}_2\text{N-3}$ represents an interesting case where all C atoms occupy one fcc sublattice and B and N atoms occupy another. It contains only N-C and B-C bonds, the same weak links as in $\text{BC}_2\text{N-1}$; however, it has a slightly different charge distribution due to differences in local bonding environments, resulting in an enhanced peak stress of 46.3 GPa. $\text{BC}_2\text{N-4}$ and $\text{BC}_2\text{N-5}$ contain one B-B bond and one N-N bond, respectively. In $\text{BC}_2\text{N-4}$ the N-C bonds are still the weakest link and dominate the deformation process; combined with the weak B-B bonds in the same weak direction, it leads to a small peak stress of 21.9 GPa. In $\text{BC}_2\text{N-5}$ the broken N-N bonds significantly reduce the bond density in the $[\bar{1}\bar{1}\bar{1}]$ direction, resulting in the breaking of the remaining C-C bonds at a small (about 3%) strain with a peak stress of only 6 GPa. These results demonstrate that $\text{BC}_2\text{N-2}$ has the highest overall strength and, therefore, should be the hardest among all the cubic BC_2N phases.

A careful examination of the bonding structures reveals that along the weak directions there is always a *global alignment* of the weak bonds that set off collective

bond-breaking processes at large strains. In $\text{BC}_2\text{N-1}$, the weakest N-C bonds form zigzag chains in the (101) plane; the B-C bonds form separate (parallel) zigzag chains in the same plane. Under strain, the weaker N-C chains break first. In $\text{BC}_2\text{N-2}$, the weakest link is composed of the zigzag chains with alternating weak N-C and stronger B-N bonds in the $(\bar{1}01)$ plane (see Fig. 3). The weak N-C bonds start to break up first under strain (see Fig. 2), which leaves the B-N bonds vulnerable. Consequently, the B-N bonds also start to stretch and eventually break up before the weaker C-B bonds that are aligned in the same direction along the applied strain but are not part of the weak chain link. The stronger B-N bonds in this weak chain enhances the strength of $\text{BC}_2\text{N-2}$ over that of a pure N-C chain as in $\text{BC}_2\text{N-1}$. The situation in other structures is similar. In particular, in $\text{BC}_2\text{N-5}$ the strongest C-C bonds break before the weaker B-C bonds since the former is part of the overall weak -N-N-C-C- chain in the $[\bar{1}\bar{1}\bar{1}]$ direction. These results highlight the deformation mechanism in cubic BC_2N phases and provide an explanation for the experimentally measured high values of hardness for cubic BC_2N nanocomposites [5] where grains of cubic BC_2N crystallites of a few nanometers in diameter are embedded in an amorphous carbon matrix. In such an environment weak bonds can never line up in any direction for more than a few bond lengths. The surface strain and interface with the structurally very strong amorphous carbon matrix are expected to enhance the structural strength. All these impose limits on the collective structural deformation. Furthermore, random orientations of BC_2N nanocrystallites also increase the overall strength due to the contributions from other stronger (e.g., $\langle 100 \rangle$ and $\langle 110 \rangle$) directions. However, BC_2N with the zinc blende structure and randomly distributed B, C, and N atoms are not expected to enhance hardness since the random bond distribution will inevitably introduce N-N and/or B-B bonds that are energetically

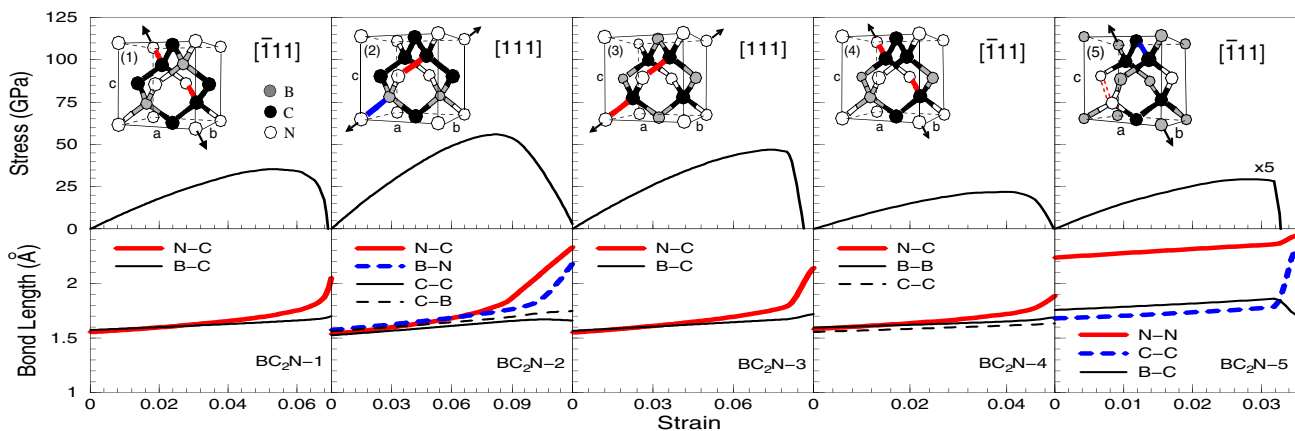


FIG. 2 (color online). Calculated stress-strain curves for five BC_2N structures (their zinc-blende-structured unit cells are shown) with the minimum peak stress (the direction of corresponding tensile strain in each case is indicated by arrows). Also shown are the bond length versus strain results (only the bonds in the direction of the tensile strain are plotted).

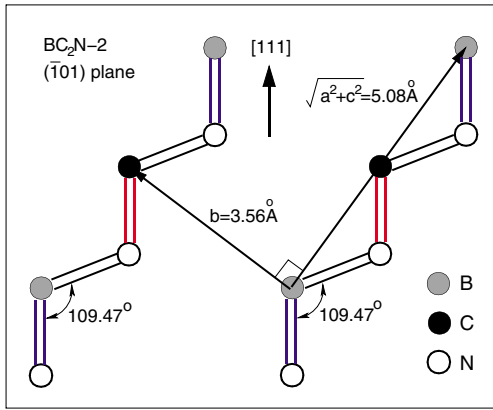


FIG. 3 (color online). The bonding structure in the $(\bar{1}01)$ plane of $\text{BC}_2\text{N-2}$, showing the weak links in the $[111]$ direction.

cally unfavorable and result in broken bonds and reduced density [10]. All these will reduce material strength. Therefore, synthesis of nanocomposites instead of the traditional crystalline form of material may be a more fruitful route in the quest for new superhard materials.

We have performed dynamic phonon calculations on the strained (up to the maximum stress) structure of $\text{BC}_2\text{N-2}$ and found no phonon instabilities. This lack of acoustic phonon softening near the zone center up to the peak stress is the result of the low symmetry caused by the structural distortion. This affirms the assignment of $\text{BC}_2\text{N-2}$ as the hardest pure phase cubic BC_2N structure. Nanocomposites with $\text{BC}_2\text{N-2}$ as the core nanocrystallites should result in the best structural character. It remains unclear whether the experimentally prepared samples [5] indeed contain $\text{BC}_2\text{N-2}$, instead of $\text{BC}_2\text{N-1}$ as previously thought [6–10]. Another important open issue is how to better design synthesis routes to distinguish $\text{BC}_2\text{N-1}$ and $\text{BC}_2\text{N-2}$.

In summary, we have performed first-principles studies of the ideal strength of cubic BC_2N . The calculations reveal that (i) most cubic BC_2N phases exhibit significant anisotropy in their ideal strengths in body diagonal directions due to compositional variations despite the overall cubic symmetry, (ii) the bonding characters at large strains are different from those near the equilibrium structure, and (iii) global alignment of weak bonds dictates the weak direction that sets the limit on the ideal strength. These factors explain why cubic BC_2N is weaker than cubic BN despite the fact that the former has the higher elastic parameters. The optimal BC_2N structure is predicted to be behind diamond and cubic BN in hardness. The higher hardness values measured on cubic BC_2N nanocomposites are most likely due to the nanocrystalline size (surface/interface) effect and the bonding with

the amorphous carbon matrix in these composite materials. Their effects on the hardness of nanocomposite materials need further investigation.

We thank Y.S. Zhao for discussions on experiments. H.S. acknowledges discussions on the equilibrium structures of BC_2N with M.L. Cohen and S.G. Louie. This work was supported by the DOE under Cooperative Agreement DE-FC52-01NV14049 at UNLV. H.S. was also supported by the NNSF of China under Grant No. 10274050 and the High Performance Computing Center at Shanghai Jiao Tong University.

- [1] S. Nakano, *et al.*, *Chem. Mater.* **6**, 2246 (1994).
- [2] E. Knittle *et al.*, *Phys. Rev. B* **51**, 12 149 (1995).
- [3] T. Komatsu *et al.*, *J. Mater. Chem.* **6**, 1799 (1996).
- [4] V.L. Solozhenko *et al.*, *Appl. Phys. Lett.* **78**, 1385 (2001).
- [5] Y. Zhao *et al.*, *J. Mater. Res.* **17**, 3139 (2002).
- [6] W.R.L. Lambrecht and B. Segall, *Phys. Rev. B* **40**, 9909 (1989).
- [7] Y. Tateyama *et al.*, *Phys. Rev. B* **55**, R10 161 (1997).
- [8] J.C. Zheng *et al.* *J. Phys. Condens. Matter* **11**, 927 (1999).
- [9] R.Q. Zheng *et al.*, *Appl. Phys. Lett.* **75**, 2259 (1999).
- [10] H. Sun *et al.*, *Phys. Rev. B* **64**, 094108 (2001).
- [11] F. Gao *et al.*, *Phys. Rev. Lett.* **91**, 015502 (2003).
- [12] A. Kelly and N.H. Macmillan, *Strong Solids* (Clarendon, Oxford, 1986), 3rd ed., p. 1.
- [13] J.W. Morris, Jr. *et al.*, in *Phase Transformations and Evolution in Materials*, edited by P.E. Turchi and A. Gonis (TMS, Warrendale, PA, 2000), p. 187.
- [14] S.H. Jhi *et al.*, *Phys. Rev. Lett.* **87**, 075503 (2001).
- [15] J. Li and S. Yip, *Comput. Model. Eng. Sci.* **3**, 219 (2002).
- [16] D.M. Clatterbuck *et al.*, *Phys. Rev. Lett.* **91**, 135501 (2003).
- [17] J. Ihm, A. Zunger, and M.L. Cohen, *J. Phys. C* **12**, 4409 (1979).
- [18] D.M. Ceperley and B.J. Alder, *Phys. Rev. Lett.* **45**, 566 (1980).
- [19] M.L. Cohen, *Phys. Scr.* **T1**, 5 (1982).
- [20] N. Troullier and J.L. Martins, *Phys. Rev. B* **43**, 1993 (1991).
- [21] J.P. Perdew and A. Zunger, *Phys. Rev. B* **23**, 5048 (1981).
- [22] B.G. Pfommer *et al.*, *J. Comput. Phys.* **131**, 233 (1997).
- [23] H.J. Monkhorst and J.D. Pack, *Phys. Rev. B* **13**, 5188 (1976).
- [24] D. Roundy, *et al.* *Philos. Mag. A* **81**, 1725 (2001).
- [25] D. Roundy, *et al.* *Phys. Rev. Lett.* **82**, 2713 (1999).
- [26] X. Gonze, *Phys. Rev. B* **55**, 10 337 (1997); X. Gonze and C. Lee, *ibid.* **55**, 10 355 (1997).
- [27] Z.C. Pan, H. Sun, and C.F. Chen, *Phys. Rev. B* (to be published).
- [28] R.H. Telling *et al.*, *Phys. Rev. Lett.* **84**, 5160 (2000).
- [29] H. Chacham and L. Kleinman, *Phys. Rev. Lett.* **85**, 4904 (2000).